Original Research

Manipulation of Image Intensity Distribution at 7.0 T: Passive RF Shimming and Focusing With Dielectric Materials

Qing X. Yang,[1]* Weihua Mao,[1] Jinghua Wang,[2] Michael B. Smith,[1] Hao Lei,[3] Xiaoliang Zhang,[4] Kamil Ugurbil,[4] and Wei Chen[4]

Purpose: To investigate the effects of high dielectric material padding on RF field distribution in the human head at 7.0 T, and demonstrate the feasibility and effectiveness of RF passive shimming and focusing with such an approach.

Materials and Methods: The intensity distribution changes of gradient-recalled-echo (GRE) and spin-echo (SE) images of a human head acquired with water pads (dielectric constant = 78) placed in specified configurations around the head at 7.0 T were evaluated and compared with computer simulation results using the finite difference time domain (FDTD) method. The contributions to the B_1 field distribution change from the displacement current and conductive current of a given configuration of dielectric padding were determined with computer simulations.

Results: MR image intensity distribution in the human head with an RF coil at 7.0 T can be changed drastically by placing water pads around the head. Computer simulations reveal that the high permittivity of water pads results in a strong displacement current that enhances image intensity in the nearby region and alters the intensity distribution of the entire brain.

Conclusion: The image intensity distribution in the human head at ultra-high field strengths can be effectively manipulated with high permittivity padding. Utilizing this effect, the B_1 field inside the human head of a given RF coil can be adjusted to reduce the B_1 field inhomogeneity artifact associated with the wave behavior (RF passive shimming) or to locally enhance the signal-to-noise ratio (SNR) in targeted regions of interest (ROIs; RF field focusing).

Key Words: high-field MRI; RF field inhomogeneity; RF field passive shim; RF field focusing; FDTD
J. Magn. Reson. Imaging 2006;24:197–202.

INTERACTIONS BETWEEN THE HUMAN BODY and RF field in ultra-high-field human MRI systems (7.0–9.4 T) present interesting challenges for RF engineering (1,2). In the corresponding RF field frequency regime, the RF magnetic field inside a human head exhibits prominent wave behavior that destroys the otherwise homogeneous field produced by an unloaded RF coil (3–7). The electrical properties, geometry, and relative position of the sample in the coil become important factors in determining the RF field distribution inside the sample (6). In addition to sample size with respect to the wavelength of the RF field, the high dielectric permittivity (dielectric constant) of human tissues is a key physical parameter that contributes to the wave phenomenon. Consequently, adjustment of RF field distribution inside the sample and the coupling between the sample and coil can be facilitated with high permittivity materials. Studies performed at 3.0 and 4.0 T indicate that the RF field distribution can be altered by changing the coil loading (8,9). With increasing RF field frequency (up to 300 MHz at 7.0 T), this effect is drastically amplified. In this study, experimental results and computer simulations demonstrate that the RF field distribution at 300 MHz in a human head can be drastically altered with water padding. The results provide experimental and theoretical evidence that the RF field inside the human body at high fields can be effectively adjusted to a desirable distribution by proper placement of dielectric materials of certain geometries between the coil and sample. By this means, passive shimming of the RF field can be performed.

THEORY

For conductive dielectric materials, such as human brain tissues, the RF field inside the sample is per-

[1]Center for NMR Research, Department of Radiology, Pennsylvania State University College of Medicine, Hershey, Pennsylvania, USA.
[2]Department of Diagnostic Radiology, School of Medicine, Yale University, New Haven, Connecticut, USA.
[3]State Key Lab of Magnetic Resonance, WuHan Institute of Physics and Mathematics, Chinese Academy of Science, Hubei, China.
[4]Center for MR Research, Department of Radiology, School of Medicine, University of Minnesota, Minneapolis, Minnesota, USA.
Contract grant sponsor: NIH; Contract grant number: R01EB000454.
Presented in part at the 9th Annual Meeting of ISMRM, Glasgow, Scotland, 2001.
*Address reprint requests to: Q.X.Y., Center for NMR Research, NMR/MRI Building, Department of Radiology H066, Pennsylvania State University College of Medicine, 500 University Drive, Hershey, PA 17033. E-mail: qyang@psu.edu
Received February 24, 2005; Accepted March 22, 2006.
DOI 10.1002/jmri.20603
Published online 5 June 2006 in Wiley InterScience (www.interscience.wiley.com).

turbed by conductive ($\mathbf{J}_c$) and displacement ($\mathbf{J}_d$) currents according to Maxwell's equation:

$$\nabla \times \mathbf{H} = \mathbf{J}_c + \mathbf{J}_d = \sigma\mathbf{E} + i\varepsilon_r\varepsilon_0\omega\mathbf{E} \quad (1)$$

where $\mathbf{H}$ is the magnetic field, $\mathbf{E}$ is the electric field, ω is the angular frequency, ε_r is the relative electric permittivity (dielectric constant), ε_0 is the electric permittivity in vacuum, σ is the conductivity of the sample, and $i = \sqrt{-1}$ is the complex unit that introduces a 90° phase difference between the conductive current and the displacement current (10). The conductive current induced by the RF field (eddy current) leads to a rapid decay of the RF field in the tissue as a function of depth from the surface of the body, while the displacement current acts as a secondary field source that facilitates RF wave propagation through the body. For brain tissue, although the conductivity increases while permittivity decreases with the frequency of the RF field, both $\mathbf{J}_d$ and $\mathbf{J}_c$ increase in the brain with the frequency (11). Because $\mathbf{J}_d$ is proportional to the RF field frequency, the displacement current increases faster than the eddy current (6). Thus, a strong RF field can be formed inside the human body despite increased tissue conductivities and eddy currents at high field strengths. Concomitantly, since the wavelength is inversely proportional to $\sqrt{\varepsilon_r}$ (15), the high dielectric constant also shortens the wavelength of the RF field such that it is comparable to the physical dimension of human-size samples. For example, the wavelength in the human brain at 300 MHz is about 13 cm, which is close to the size of an adult human brain. Under such geometrical conditions, the phase distribution of the RF field from a given source becomes spatially dependent across the sample. The observed inhomogeneous RF field distribution is the interference pattern of the RF waves from various sources, such as coil elements and boundaries between tissues with different dielectric constants. Thus, the high tissue permittivity plays a critical role in the emergence of such RF field wave behavior in the human sample at high field strengths. This suggests that it is possible to use high permittivity materials to alter the displacement current distribution so that the RF field can be adjusted to a desired distribution in a targeted region.

MATERIALS AND METHODS

The gradient-recalled-echo (GRE) and spin-echo (SE) human brain images were acquired using a 7.0 T whole-body imaging system (Magnex Scientific Ltd. magnet with Varian NMR console) using a quadrature TEM head resonator for both transmitter and receiver with slice thickness = 5 mm, matrix size = 256 × 256 and FOV = 25 × 25 cm^2. The images were acquired with TR/TE = 100 msec/4 msec for GRE images, and TR/TE = 3000 msec/40 msec for SE images. The nominal flip angles were 20° for the GRE sequence, and 90° and 180° for the SE sequence. The flip angles were calibrated with an experimentally determined nominal 90° angle that produced maximum signal from the sample with a single nonselective excitation. To empirically examine the effect of dielectric loading on the image intensity distribution, we placed water pads containing 200–400 mL of double-distilled water around each subject's head at various locations. Two shimming configurations were applied for this study. One was a single distilled-water pad that conformed to the subject's forehead above the eye level with a length, width, and thickness of about 16 cm, 6 cm, and 4 cm, respectively. Another configuration was four distilled-water pads of the same dimensions that were formed in a circle around the head. The images were acquired with identical parameters before and after the water pads were removed. However, the 90° and 180° flip angles were adjusted following retuning of the coil after water pads were removed. The subjects remained in the magnet while the water pads were removed and the tuning and matching of the RF coil were adjusted. A total of four human studies were performed for this investigation. Informed consent, as approved by the institutional review board, was obtained from all of the human subjects prior to the MRI studies.

To understand the physical underpinning of the dielectric loading effect, we performed a numerical analysis with the finite difference time domain (FDTD) method using XFDTD software (REMCOM Corp., State College, PA, USA). The numerical calculation was carried out with a 12-element TEM coil loaded with a three-dimensional human head model consisting of 23 different tissue types with a 5-mm isotropic resolution (12). Distilled water was simulated by assigning the medium with $\sigma = 0$ and $\epsilon_r = 78$. The resonance frequency of the TEM coil model was first tuned to 300MHz by adjusting the length of the inner conductors and the relative permittivity between inner and outer conductors of the coil elements. Subsequently, a unit voltage at 300 MHz was applied on each of the 12 TEM coil elements. The phases of the voltage source followed the azimuthal angle positions of the coil element to generate an ideal quadrature sinusoidal current distribution. The magnitudes of the positive (B_1^+) and negative (B_1^-) circularly polarized magnetic field components were calculated. The signal intensity (SI) for GRE image was then calculated as

$$SI \propto \sin(V\gamma\tau|B_1^+|)|B_1^-| \quad (2)$$

where V is a dimensionless normalization factor proportional to the coil driving voltage, γ is the gyromagnetic ratio, and τ is the duration of the RF pulse (5). The corresponding $\mathbf{J}_d$ and $\mathbf{J}_c$ were determined using Eq. [1].

RESULTS

Figure 1 shows the experimental and simulated GRE sagittal brain images with and without water padding at 7.0 T. The image in Fig. 1a exhibits a typical intensity distribution in a human head at high field strengths, with a prominent bright region in the center of the head. As shown in Fig. 1b, when water padding is placed on the forehead, the center bright region appears to be "drawn" to the superior-frontal brain area near the padding, accompanied by a considerable signal decrease in the posterior region. Figure 1c and d illustrate the cor-

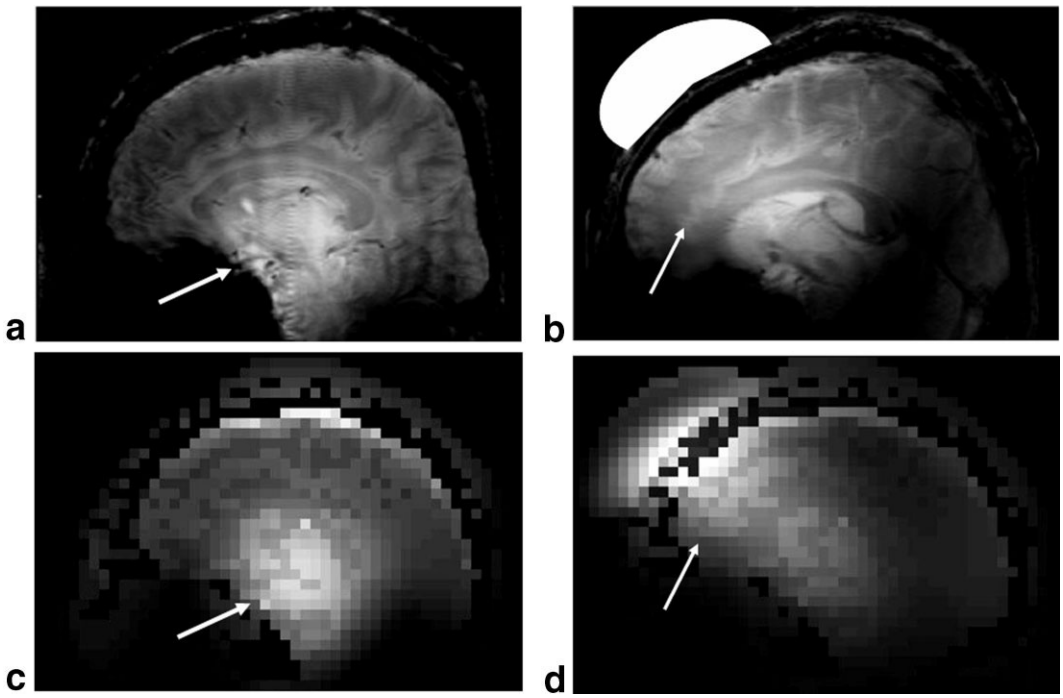

Figure 1. Sagittal GRE head images acquired at 7.0 T without (**a**) and with (**b**) the water pad and the corresponding calculated images (**c** and **d**). The prominent bright region in the center of the human head, indicated by the arrows in images a and c, is shifted to the brain area closer to the water pad in images b and d. In order to properly window the image intensity, the water pad in the experimental image in b is removed and represented with a drawing. The simulated GRE images reproduce the characteristics of the intensity distribution changes of the experimental image.

responding calculated GRE images weighted with relative water content of the brain model so that basic brain structures can be visualized. The computer simulation results closely reproduce the relative image intensity distributions in both experimental conditions. Note that the signal intensity near the water padding in Fig. 1d appears appreciably stronger than the center bright spot in Fig. 1c, indicating a local signal enhancement by the dielectric padding. The remarkable intensity distribution change by the water padding demonstrates the effectiveness of using materials with a high dielectric constant to manipulate the field distribution inside the human brain at high field strengths.

Figure 2 shows two sets of SE images from the same

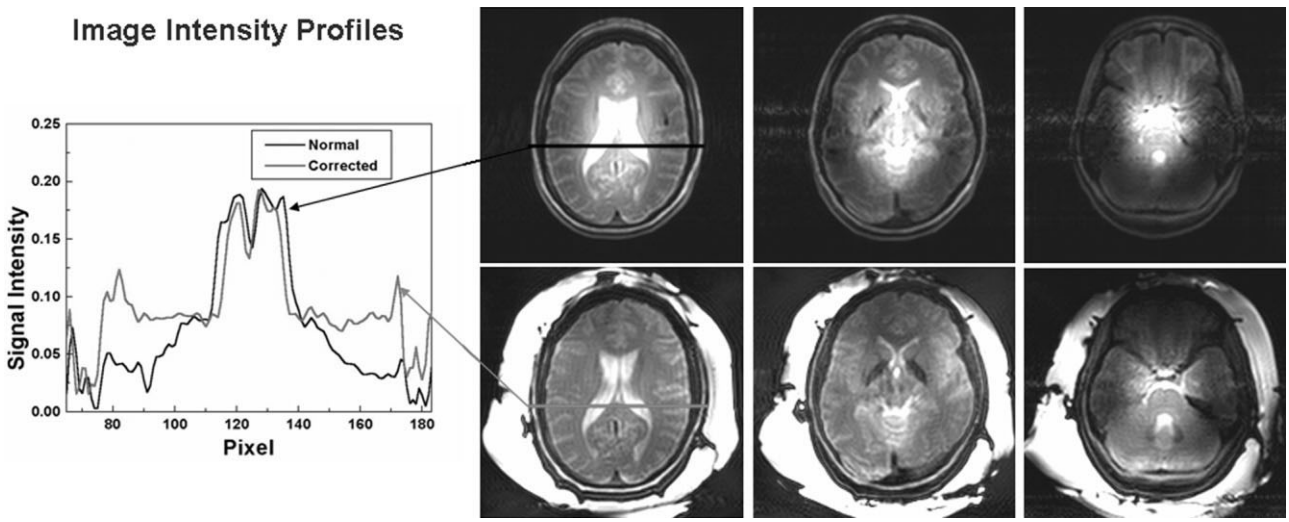

Figure 2. Axial SE images of a human head acquired at 7.0 T without (top row) and with (bottom row) water pads. The image intensity acquired with water pads around the head from the same subject using identical experimental parameters becomes more uniform within the same tissue type over the image slices. The bright areas surrounding the head are the images of water pads. The signal intensity profiles on the left show a quantitative signal intensity comparison along the horizontal lines in the images of the same slice acquired with and without the pads.

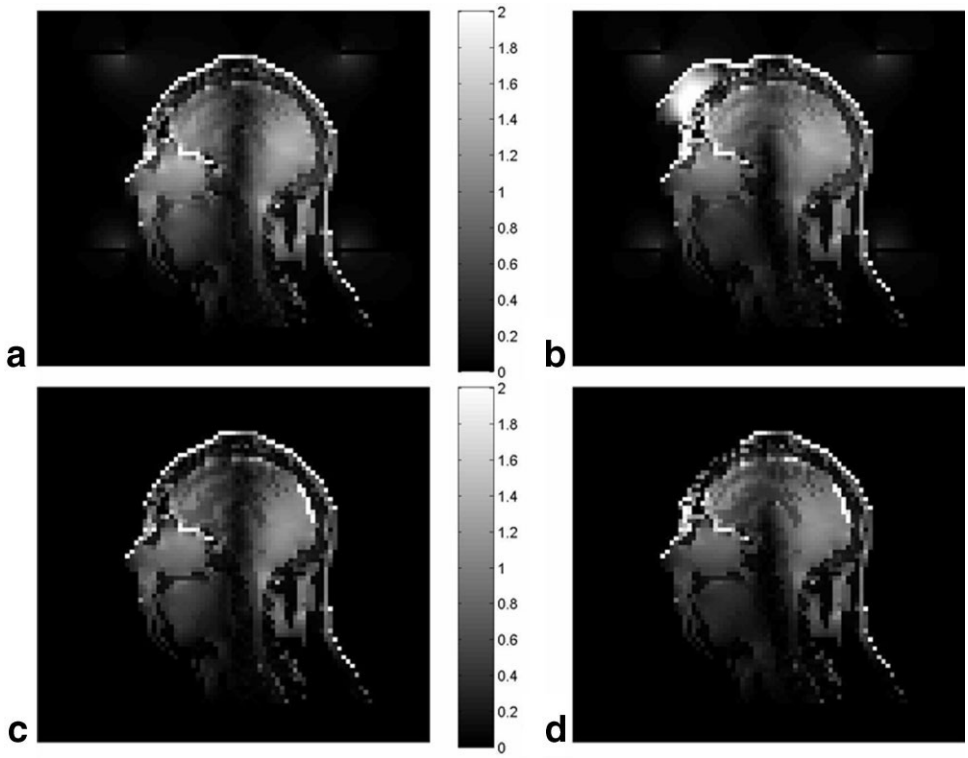

Figure 3. The z-component of displacement current density (**a** and **b**) and conductive current density (**c** and **d**) (A/m^2) without (left column) and with (right column) the dielectric pad.

axial slices. With the SE method the B_1 field inhomogeneity is exaggerated because of the additional 180° RF pulse in the SE sequence. The images acquired without water padding in the top row exhibit an extraordinarily large image intensity variation characterized by a hyperintense region in the brain center surrounded by a dark peripheral area. This intensity characteristic becomes more prominent in the image sections in the inferior brain region. The image intensity of the same tissue type in the center region can be twice as strong as that in the dark peripheral region. With such nonuniform image intensity, the utilization of SE images at high field strengths is severely limited. The images in the bottom row show the same brain slices acquired when four water pads are placed symmetrically around the head above the eye level. The strong image intensity in the central brain region is significantly leveled out, rendering a uniform signal intensity distribution over the entire image slice. To illustrate this effect quantitatively, the plot on the left shows the image intensity across the horizontal lines as indicated in the axial images without and with the water padding. As indicated in the plot, a more uniform image intensity distribution was achieved with dielectric material around the head, which allowed for a better SE image at 7.0 T.

To understand the physical underpinning of the dielectric padding effect on the B_1 field distribution, we decomposed and evaluated the sources of the B_1 field, $\mathbf{J}_c$ and $\mathbf{J}_d$, separately. Figure 3 shows the z-components of $\mathbf{J}_d$ and $\mathbf{J}_c$ that generate the transverse B_1 field in the mid-sagittal plane without and with a dielectric pad on the forehead. The most conspicuous feature in Fig. 3a and c is a prominent dark band along the axis of symmetry of the coil, which indicates low current intensity distributions in this region. The current intensity directions on each side of the dark band are opposite, which is consistent with the observed strong B_1 field distribution in the center of the brain. With a placement of high dielectric constant padding, both $\mathbf{J}_d$ and $\mathbf{J}_c$ distributions were altered considerably. In particular, a strong and highly concentrated displacement current distribution was induced in the dielectric pad. This introduced a local current source that resulted in a stronger B_1 field in the nearby brain region, as shown in Fig. 2. The current intensities in the dark bands in the superior brain region were also increased significantly, yielding a completely different B_1 field distribution.

DISCUSSION

RF field inhomogeneity at high fields has long been observed as a well-known "bright center spot" in human brain images obtained on 3 and 4 T imaging systems (13–18), as well as in human-body-size phantom images taken at 1.5 T (19). As demonstrated by the human brain SE images in Fig. 2, this effect is drastically intensified because of a stronger B_0 field strength. This phenomenon has been considered to result from the wave behavior of the RF field. The fundamental factor for the observed wave behavior, however, can be attributed to the high dielectric constant of human or biological tissues. First, the wavelength of the RF field is approximately and inversely proportional to the square root of dielectric constant. Because of the high dielec-

tric constant of the human brain tissues, the wavelength of the RF field in human brain at 300 MHz is close to the size of an adult human brain. Under this condition a strong wave behavior arises, causing a severe RF field inhomogeneity. Second, as shown in Eq. [1], the displacement current is a secondary source for the B_1 field propagation. The RF wave propagation depends on the displacement current that is directly proportional to the dielectric constant. Thus, the high tissue permittivity is a key factor for the prominent wave behavior seen in high-field MRI. Although the dielectric constant distribution in human samples cannot be changed easily, the RF field can be manipulated by altering the dielectric constant distribution between the sample and an RF coil. As demonstrated in Fig. 1, the simple placement of a water pad that introduced a strong local $\mathbf{J}_d$ source and altered coupling between the coil and the head dramatically changed the RF field distribution inside the human head.

Our experiences with the TEM coil on a 7.0 T human imaging system and computer simulations indicated that the current distribution in the coil elements could be perturbed by sample loading (20). This raises the question as to whether the current distribution in the coil conductors could be altered by a dielectric loading, such as water pads, which may in turn contribute to the observed image intensity changes. This issue was addressed carefully in a previous study (20) in which the image intensities with and without dielectric padding were calculated twice: one with an ideal sinusoidal current distribution, as in our current computer simulation, and one with the current distribution significantly perturbed by the water pad simulated using two power input ports, as in the current experiment. The results showed that image-intensity changes due to water padding are similar in these two cases. Thus, the dominant cause for the image intensity change is $\mathbf{J}_d$ in the water pads. Experimentally, the images with and without water pads were acquired after the coil's tuning and matching were carefully adjusted, which may partially compensate for the perturbation of the coil current distribution by the water pads.

In our experiment we used water as a dielectric medium to demonstrate the described effect. However, from a technical point of view, water is not a suitable high-dielectric material for this purpose because it produces a strong signal that saturates the receiver and deceases the dynamic range of the digitizer, and its movements and geometry are difficult to control. Solid-state materials with a high dielectric constant and low conductivity are more advantageous and may be used for future developments. To utilize dielectric material for passive RF shimming, a systematic investigation with the aid of computer modeling is necessary in order to address these technical issues and to devise an optimization routine for a desirable B_1 field distribution.

The strong effect of the water padding on the RF field distribution demonstrated in this experiment has an important practical significance. The RF field inhomogeneity has been a critical limitation for effective utilization of ultra-high-field MRI systems (3). Various RF coil designs, image acquisitions, and postprocessing approaches have been proposed to reduce such artifacts (21–26). The results of this experiment suggest an effective way to adjust the RF field distribution inside the sample. As demonstrated in Figs. 1 and 2, similarly to the passive shimming of the static magnetic field, the RF field for a given coil and sample configuration can also be "shimmed" passively with placements of the dielectric material between the sample and the coil. RF field shimming with dielectric material is effective and versatile. As indicated in the Fig. 1, one can easily move the high-SNR region from one brain region to another by placing water pads at a certain location. This allows us to manipulate the RF field to achieve not only a more homogeneous RF field distribution, but also a focused high-signal-intensity area in an ROI. The latter approach can be used to enhance SNR in an ROI for functional MRI (fMRI) studies and other localized investigations, such as localized spectroscopy. The RF shimming and focusing with dielectric material illustrated in this study can be integrated directly into RF coil designs. The investigations at 7.0 T demonstrate that parallel-imaging methods that utilize inhomogeneous RF field for spatial encoding would most likely offer a solution for RF field engineering at high fields. The RF shimming and focusing with dielectric materials can be utilized with the development and optimization of multicoil systems for parallel imaging at high fields (27,28). Based on the principles demonstrated in this study, more deliberate engineering methods can be devised to produce desirable RF field distributions at various field strengths.

In conclusion, the high dielectric constant in biological tissues leads to the pronounced RF field wave behavior that destroys the field homogeneity in the human body at high fields. Experimental and computer simulation results at 7.0 T demonstrate that one can effectively manipulate the MR image intensity distribution in the human head with a given volume coil by placing water pads around the head. The high permittivity of water results in a strong displacement current that enhances image intensity in the nearby region and alters the overall intensity distribution. Utilizing this effect, one can adjust the B_1 field of a given RF coil inside the human head to remove the field inhomogeneity artifact associated with the wave behavior (RF passive shimming) or to locally enhance SNR in a targeted ROI (RF field focusing). A thorough understanding of this phenomenon may lead to an effective approach for RF field engineering in high-field MRI.

REFERENCES

1. Abduljalil AM, Kangarlu A, Zhang X, et al. Acquisition of human multislice MR images at 8 Tesla. J Comput Assist Tomogr 1999;23: 335–340.
2. Vaughan JT, Garwood M, Collins CM, et al. 7T vs. 4T: RF power, homogeneity, and signal-to-noise comparison in head images. Magn Reson Med 2001;46:24–30.
3. Beck BL, Jenkins KA, Padgett K, et al. Observation of B1 inhomogeneities on large biological samples at 11.1 Tesla. In: Proceedings of the 11th Annual Meeting of ISMRM, Toronto, Canada, 2003. p 716.
4. Hoult DI, Phil D. Sensitivity and power deposition in a high-field imaging experiment. J Magn Reson Imaging 2000;12:46–67.

5. Collins CM, Yang QX, Wang JH, et al. Different excitation and reception distributions with a single-loop transmit-receive surface coil near a head-sized spherical phantom at 300 MHz. Magn Reson Med 2002;47:1026–1028.
6. Yang QX, Wang J, Zhang X, et al. Analysis of wave behavior in lossy dielectric samples at high field. Magn Reson Med 2002;47:982–989.
7. Wang J, Yang QX, Zhang X, et al. Polarization of the RF field in a human head at high field: a study with a quadrature surface coil at 7.0 T. Magn Reson Med 2002;48:362–369.
8. Foo TK, Hayes C, Kang YW. Reduction of RF penetration effects in high field imaging. Magn Reson Med 1992;23:287–301.
9. Alsop DC, Connick TJ, Mizsei G. A spiral volume coil for improved RF field homogeneity at high static magnetic field strength. Magn Reson Med 1998;40:49–54.
10. Johnk CT. Engineering electromagnetic fields and waves. New York: Wiley; 1988. p 363.
11. Gabriel C. Compilation of the dielectric properties of body tissues at RF and microwave frequencies. AL/OE-TR-1996-0037. Brooks Air Force Base, TX: Air Force Material Command; 1996.
12. Collins CM, Smith MB. Calculations of B1 distribution, SNR, and SAR for a surface coil adjacent to an anatomically-accurate human body model. Magn Reson Med 2001;45:692–699.
13. Wen H, Jaffer FA, Denison TJ, et al. The evaluation of dielectric resonators containing H_2O or D_2O as RF coils for high-field MR imaging and spectroscopy. J Magn Reson Ser B 1996;110:117–123.
14. Bomsdorf H, Helzel T, Kunz D, et al. Spectroscopy and imaging with a 4 tesla whole-body MR system. NMR Biomed 1988;1:151–158.
15. Tofts PS. Standing waves in uniform water phantoms. J Magn Reson Ser B 1994;104:1–5.
16. Vaughan JT, Hetherington HP, Otu JO, et al. High frequency volume coils for clinical NMR imaging and spectroscopy. Magn Reson Med 1994;32:206–218.
17. Sled JG, Pike GB. Standing wave and RF penetration artifacts caused by elliptic geometry: an electrodynamics analysis. IEEE Trans Med Imaging 1998;17:653–662.
18. Collins CM, Liu W, Schreiber W, Yang QX, Smith MB. Central brightening due to constructive interference with, without, and despite dielectric resonance. J Magn Reson Imaging 2005;21:192–196.
19. Glover GH, Hayes CE, Helc NJ, et al. Comparison of linear and circular polarization for magnetic resonance imaging. J Magn Reson 1985;64:255–270.
20. Mao W, Smith MB, Yang QY. Simulation on passive RF shimming in ultra-high field with high permittivity dielectrics. In: Proceedings of the 13th Annual Meeting of ISMRM, Miami Beach, FL, USA, 2005. p 821.
21. Adriany G, Van de Moortele P, Wiesinger F, et al. Transceive stripline arrays for ultra high field parallel imaging applications. In: Proceedings of the 11th Annual Meeting of ISMRM, Toronto, Canada, 2003. p 474.
22. Saekho S, Boada FE, Noll DC, et al. B1 inhomogeneity compensation using 3D tailored RF pulses. In: Proceedings of the 11th Annual Meeting of ISMRM, Toronto, Canada, 2003. p 717.
23. Cohen MS, DuBois RM, Zeineh MM. Rapid and effective correction of RF inhomogeneity for high field magnetic resonance imaging. Hum Brain Mapp 2000;10:204–211.
24. Han C, Hatsukami TS, Yuan C. A multi-scale method for automatic correction of intensity non-uniformity in MR images. J Magn Reson Imaging. 2001;13:428–436.
25. Thesen S, Krueger G, Mueller E, Compensation of dielectric resonance effects by means of composite excitation pulses. In: Proceedings of the 11th Annual Meeting of ISMRM, Toronto, Canada, 2003. p 715.
26. Zhang X, Ugurbil K, Chen W. A microstrip transmission line volume coil for human head MR imaging at 4T. J Magn Reson 2003; 161:242–251.
27. Sodickson DK, Manning WJ. Simultaneous acquisition of spatial harmonics (SMASH): fast imaging with radiofrequency coil arrays. Magn Reson Med 1997;38:591–603.
28. Pruessmann KP, Weiger M, Scheidegger MB, et al. SENSE: sensitivity encoding for fast MRI. Magn Reson Med 1999;42:952–962.